

Analytic pulse design for selective population transfer in many-level quantum systems: Maximizing the amplitude of population oscillations

Duje Bonacci*

Physical Chemistry Department, R. Bošković Institute, Bijenička 54, 10000 Zagreb, Croatia

(Received 25 December 2003; published 29 October 2004)

State-selective preparation and manipulation of discrete-level quantum systems such as atoms, molecules, or quantum dots is the ultimate tool for many diverse fields such as laser control of chemical reactions, atom optics, high-precision metrology, and quantum computing. Rabi oscillations are one of the simplest, yet potentially quite useful mechanisms for achieving such manipulation. Rabi theory establishes that in the two-level systems resonant drive leads to the periodic and complete population oscillations between the two system levels. In this paper an analytic optimization algorithm for producing Rabi-like oscillations in the general discrete many-level quantum system is presented.

DOI: 10.1103/PhysRevA.70.043413

PACS number(s): 32.80.Qk, 03.65.Sq

I. INTRODUCTION

During the past 20 years a number of methods has been devised for state-selective preparation and manipulation of discrete-level quantum systems [1–5]. However, simple population oscillations, induced by a resonant driving pulse have received negligible attention as a prospective population manipulation method. This might be attributed to two reasons. The first is that Rabi theory is based on the rotating-wave approximation (RWA), and all attempts to generalize it without RWA (e.g., Refs. [6–8]) are mathematically very involved. The second is that no attempt has been made to analytically generalize the original Rabi theory beyond two-level systems.

In this paper an analytic extension of Rabi theory to transitions in many-level systems is presented. The aim is to “design” a driving pulse of the form

$$F(t) = F_0 m(t) \cos[\omega(t)t] \quad (1)$$

by establishing analytical optimization relations between its parameters: maximum pulse amplitude F_0 , pulse envelope shape $m(t)$, and time dependent carrier frequency $\omega(t)$. The goal of this enterprise is twofold. The first is to achieve as complete as possible transfer of population between two selected states of the system. The second is to make this transfer as rapid as possible. These two requirements, however, are contradictory; population transfer can be accelerated by using a more intense drive, but at the same time a stronger drive increases involvement of remaining system levels in population dynamics and hence deteriorates population transfer between a selected pair of levels.

In this paper it is shown how, for a pulse of arbitrary shape and duration $m(t)$, the drive frequency can be analytically optimized to maximize the population transfer amplitude between selected two levels. In other words, Rabi oscillation theory is reformulated for the case of a many-level system driven by an arbitrary modulated pulse.

II. THEORETICAL ANALYSIS

All calculations in this section are done in a system of units in which $\hbar = 1$.

A. Calculation setup

A quantum system with N discrete stationary levels with energies E_i ($i = 1, \dots, N$) is considered. The system is driven by a time dependent perturbation given in Eq. (1). In the interaction picture, the dynamics of the system obeys the Schroedinger equation

$$\frac{d}{dt} \mathbf{a}(t) = -i \hat{\mathbf{V}}(t) \mathbf{a}(t), \quad (2)$$

where $\mathbf{a}(t)$ is a vector of time-dependent expansion coefficients $a_1(t), \dots, a_N(t)$. The $N \times N$ matrix $\hat{\mathbf{V}}(t)$ describes interaction between the system and perturbation. Explicitly, its elements are given by

$$V_{ij}(t) = \frac{F_0 \mu_{ij}}{2} m(t) [e^{is_{ij}(\omega(t) - \omega_{ij})t} + e^{-is_{ij}(\omega(t) + \omega_{ij})t}]. \quad (3)$$

μ_{ij} is the transition moment between the i th and the j th levels induced by the perturbation. $s_{ij} = \text{sign}(E_i - E_j)$ and $\omega_{ij} = |E_i - E_j|$ are, respectively, the sign and the magnitude of the resonant frequency for the transition between the i th and the j th level.

The aim is to induce population transfer between two arbitrarily selected levels, designated by α and β , directly coupled by the perturbation (i.e., such that $\mu_{\alpha\beta} \neq 0$). To simplify equations, the time variable t is rescaled to τ , with transformation between the two given by

$$d\tau = \frac{F_0 \mu_{\alpha\beta}}{2} m(t) dt. \quad (4)$$

Then with the following substitutions:

$$f_{ij}(\tau) = s_{ij} \frac{2}{F_0 \mu_{\alpha\beta}} [\omega(t) - \omega_{ij}], \quad (5)$$

*Electronic address: dbonacci@irb.hr

$$g_{ij}(\tau) = s_{ij} \frac{2}{F_0 \mu_{\alpha\beta}} [\omega(t) + \omega_{ij}], \quad (6)$$

$$x(\tau) = \frac{F_0 \mu_{\alpha\beta}}{2} t(\tau), \quad (7)$$

$$R_{ij} = \frac{\mu_{ij}}{\mu_{\alpha\beta}}. \quad (8)$$

Equation (2) transforms into

$$\frac{d}{d\tau} \mathbf{a}(\tau) = -i \hat{\mathbf{W}}(\tau) \mathbf{a}(\tau), \quad (9)$$

where

$$\frac{d}{d\tau} \begin{bmatrix} a_\alpha(\tau) \\ a_\beta(\tau) \end{bmatrix} = -i \begin{bmatrix} 0 & e^{if_{\alpha\beta}(\tau)x(\tau)} + e^{-ig_{\alpha\beta}(\tau)x(\tau)} \\ e^{-if_{\alpha\beta}(\tau)x(\tau)} + e^{ig_{\alpha\beta}(\tau)x(\tau)} & 0 \end{bmatrix} \begin{bmatrix} a_\alpha(\tau) \\ a_\beta(\tau) \end{bmatrix}. \quad (11)$$

Under certain conditions (for a thorough discussion see, e.g., Ref. [9]) this equation may be simplified by introducing the RWA. Within the RWA, dynamical impact of complex exponentials $e^{\pm g_{\alpha\beta}(\tau)x(\tau)}$ is neglected and these may be eliminated from the equation. Hence, (11) reduces to

$$\frac{d}{d\tau} \begin{bmatrix} a_\alpha(\tau) \\ a_\beta(\tau) \end{bmatrix} = -i \begin{bmatrix} 0 & e^{if_{\alpha\beta}(\tau)x(\tau)} \\ e^{-if_{\alpha\beta}(\tau)x(\tau)} & 0 \end{bmatrix} \begin{bmatrix} a_\alpha(\tau) \\ a_\beta(\tau) \end{bmatrix}. \quad (12)$$

Finally, adjusting the perturbation frequency to the resonant value [$\omega(\tau) \equiv \omega_{\alpha\beta}$] results in $f_{\alpha\beta}(\tau) = 0$, and (12) reduces to

$$\frac{d}{d\tau} \begin{bmatrix} a_\alpha(\tau) \\ a_\beta(\tau) \end{bmatrix} = -i \begin{bmatrix} 0 & 1 \\ 1 & 0 \end{bmatrix} \begin{bmatrix} a_\alpha(\tau) \\ a_\beta(\tau) \end{bmatrix}. \quad (13)$$

As may be easily demonstrated by solving this simple equation, the resonant perturbation induces complete periodic transfer of the population between two levels. The time Θ (in units of τ) or T (in units of t) required for a single population oscillation is determined from

$$W_{ij}(\tau) = R_{ij} [e^{if_{ij}(\tau)x(\tau)} + e^{-ig_{ij}(\tau)x(\tau)}]. \quad (10)$$

Initial conditions for the problem of selective population transfer comprise complete population initially (at $t = \tau = 0$) contained in only one of the selected levels, either α or β . The other selected level, as well as all the remaining $N-2$ ‘‘perturbing’’ levels of the system are unpopulated at this time.

Population evolution $\Pi_i(t)$ of the i th level is determined from $\Pi_i(t) = |a_i(t)|^2$.

B. Population oscillations in the two-level system:

Recapitulation

Having in mind that $s_{ij} = -s_{ji}$, the explicit form of the general dynamical Eq. (9) in a two-level system is

$$\int_0^\Theta d\tau \equiv \frac{F_0 \mu_{\alpha\beta}}{2} \int_0^T m(t) dt = \pi. \quad (14)$$

This is a well known result which forms the basis of π -pulse theory.

C. Population oscillations in the three-level system

As will be shown in subsequent sections, the whole analytical approach to the maximization of the population oscillation amplitude in a general many-level quantum system may be reduced to discussion of a three-level system. Along with two ‘‘selected’’ levels α and β , the system now discussed contains one additional ‘‘perturbing’’ level, designated with index p . The only requirements on the system internal structure are that $\mu_{\alpha\beta}, \mu_{\beta p} \neq 0$, and $\mu_{\alpha p} = 0$. While the first two requirements are necessary, the last one does not reduce the generality of the final results to any significant extent and it is introduced for calculational convenience.

The three-level version of the dynamical Eq. (9) is

$$\frac{d}{d\tau} \begin{bmatrix} a_\alpha(\tau) \\ a_\beta(\tau) \\ a_p(\tau) \end{bmatrix} = -i \begin{bmatrix} 0 & e^{if_{\alpha\beta}(\tau)x(\tau)} + e^{-ig_{\alpha\beta}(\tau)x(\tau)} & 0 \\ e^{-if_{\alpha\beta}(\tau)x(\tau)} + e^{ig_{\alpha\beta}(\tau)x(\tau)} & 0 & 0 \\ 0 & R_{\beta p} [e^{if_{\beta p}(\tau)x(\tau)} + e^{-ig_{\beta p}(\tau)x(\tau)}] & 0 \end{bmatrix} \begin{bmatrix} a_\alpha(\tau) \\ a_\beta(\tau) \\ a_p(\tau) \end{bmatrix}. \quad (15)$$

1. The adiabatic approach and perturbing level population dynamics

In order to solve Eq. (15) two assumptions shall be made. The legitimacy of both of them may be checked retrospectively from the final solution. The first one is that the RWA may be applied for transition $\alpha \leftrightarrow \beta$ so that exponentials containing $g_{\alpha\beta}(\tau)$ may be dropped from Eq. (15). A simple way to verify this assumption's legitimacy may be done using Rabi profile plots, as described in Ref. [9]. The second is that the dynamical time scale of solutions for $a_{\alpha,\beta}(\tau)$ is much longer than that for $a_p(\tau)$. This enables one to regard $a_{\beta}(\tau)$ as a slowly changing parameter in the dynamical equation for $a_p(\tau)$. The solution to this equation, hence, may be obtained in terms of a parameter whose value needs not be known beforehand.

Introducing the first of the assumptions into (15) and reformulating it slightly, a set of two coupled differential equations is obtained

$$\frac{d}{d\tau} \begin{bmatrix} a_\alpha(\tau) \\ a_\beta(\tau) \end{bmatrix} = -i \begin{bmatrix} 0 & e^{if_{\alpha\beta}(\tau)x(\tau)} \\ e^{-if_{\alpha\beta}(\tau)x(\tau)} & 0 \end{bmatrix} \begin{bmatrix} a_\alpha(\tau) \\ a_\beta(\tau) \end{bmatrix} - iR_{\beta p} \begin{bmatrix} e^{-if_{\beta p}(\tau)x(\tau)} + e^{ig_{\beta p}(\tau)x(\tau)} \\ 0 \\ 1 \end{bmatrix} a_p(\tau), \quad (16)$$

$$\frac{d}{d\tau} a_p(\tau) = -iR_{\beta p} [e^{if_{\beta p}(\tau)x(\tau)} + e^{-ig_{\beta p}(\tau)x(\tau)}] a_\beta(\tau). \quad (17)$$

Now consider just Eq. (17). The formal solution to this equation is

$$a_p(\tau) = -iR_{\beta p} \int_0^\tau [e^{if_{\beta p}(\tau')x(\tau')} + e^{-ig_{\beta p}(\tau')x(\tau')}] a_\beta(\tau') d\tau'. \quad (18)$$

This integral cannot be precisely evaluated until the exact form of the solution $a_\beta(\tau)$ and optimized perturbation frequency $\omega(\tau)$ —through which $f_{\beta p}(\tau)$ and $g_{\beta p}(\tau)$ are defined [(5) and (6)]—are known. Certainly, these are not known before the final solution of the whole optimization procedure is obtained. However, introduction of the second assumption enables one to evaluate the partial contribution to the integral in (18) from some interval $\tau_0 < \tau' < \tau$ within which changes in all these functions are so insignificant that functions themselves may be approximated by a constant value.

The aim of the optimization procedure is effectively to eliminate the dynamical impact of the perturbing level on population transfer between the two selected levels. If this is achieved, then dynamics of subsystem (α, β) will be very similar to the dynamics of the pure two level system. Hence, the population oscillation period will be about $\Theta = \pi$, which is then the dynamical time scale for $a_{\alpha,\beta}(\tau)$. As optimizing variations of the driving frequency $\omega(\tau)$ are caused exclusively by the changes in perturbation envelope amplitude $m[t(\tau)]$ it is transparent that dynamical time scales for $f_{\beta p}(\tau)$ and $g_{\beta p}(\tau)$ are of the same order as that for $m[t(\tau)]$. The dynamical time-scale of $m[t(\tau)]$ must be of the same order as

that of $a_{\alpha,\beta}(\tau)$ or longer, for otherwise not even a single complete population transfer would be achieved. Hence, in the interval $\tau_0 < \tau' < \tau$ such that $\tau - \tau_0 \ll \pi$, the optimized functions $a_\beta(\tau')$, $f_{\beta p}(\tau')$, and $g_{\beta p}(\tau')$ may be considered constant, $a_\beta(\tau') \approx a_\beta(\tau_0)$, $f_{\beta p}(\tau') \approx f_{\beta p}(\tau)$, and $g_{\beta p}(\tau') \approx g_{\beta p}(\tau_0)$. Finally, in this interval $x(\tau')$ may be approximated by $x(\tau') \approx x(\tau_0) + \{1/m[t(\tau_0)]\}(\tau' - \tau_0)$. In several simple steps the following result is obtained:

$$a_p(\tau) \approx c(\tau_0) - s_{\beta p} \sigma_{\beta p} \frac{m[t(\tau)]}{1 - \Delta_{\beta p}(\tau)} \left[1 - \delta_{\beta p} \frac{1 - \Delta_{\beta p}(\tau)}{1 - \delta_{\beta p} \Delta_{\beta p}(\tau)} \right] \times e^{-2is_{\beta p} \omega(\tau)t(\tau)} e^{if_{\beta p}(\tau)x(\tau)} a_\beta(\tau), \quad (19)$$

where

$$\sigma_{\beta p} = \frac{F_0 \mu_{\beta p}}{2(\omega_{\alpha\beta} - \omega_{\beta p})}, \quad (20)$$

$$\delta_{\beta p} = \frac{\omega_{\alpha\beta} - \omega_{\beta p}}{\omega_{\alpha\beta} + \omega_{\beta p}}, \quad (21)$$

$$\Delta_{\beta p}(\tau) = \frac{\omega(\tau) - \omega_{\alpha\beta}}{\omega_{\beta p} - \omega_{\alpha\beta}}. \quad (22)$$

The constant term $c(\tau_0)$ includes both the $a_p(\tau_0)$ and the integration constant obtained by inserting the lower limit value τ_0 into the solution. Its exact value cannot be determined since integration cannot be analytically stretched over the whole interval from $\tau=0$ to $\tau=\Theta$. However, since $a_p(\tau=0)=0$ this constant is of the order of average value of remaining rapid complexly rotating expression, which is very nearly equal to zero.

If detuning from resonance is assumed small, the perturbation frequency may be approximated by $\omega(\tau) \approx \omega_{\alpha\beta}$ so that $\Delta_{\beta p}(\tau) \approx 0$. The obtained solution (19) then immediately provides an upper limit for the magnitude of perturbing level population

$$|\Pi_p(\tau)| \leq \sigma_{\beta p}^2 (1 + |\delta_{\beta p}|)^2. \quad (23)$$

In general $\delta_{\beta p} \ll 1$, so the whole bracket can be reduced to 1, and the maximum amplitude of the perturbing level's population is roughly $\sigma_{\beta p}^2$. Hence, this quantity may be regarded as a parameter determining the effective strength of the perturbation applied to a particular transition: if $\sigma_{\beta p}^2 \ll 1$, then the dynamical impact of level p is negligible and the perturbation may be considered weak; if $\sigma_{\beta p}^2 \sim 1$, the perturbation is very strong. This result may also be cast into a convenient quantitative form: to keep the "leakage" of the population to the perturbing level p below a certain limiting value M_p , the greatest drive intensity which may be employed is roughly

$$F_0^{\max} = \left| \frac{2(\omega_{\alpha\beta} - \omega_{\beta p})}{\mu_{\beta p}} \right| \sqrt{M_p}. \quad (24)$$

2. Optimized driving frequency

When solution (19) is plugged into Eq. (16) a single closed dynamical equation is obtained for a two-level subsystem (α, β) :

$$\frac{d}{d\tau} \begin{bmatrix} a_\alpha(\tau) \\ a_\beta(\tau) \end{bmatrix} = -i \begin{bmatrix} 0 & e^{if_{\alpha\beta}(\tau)x(\tau)} \\ e^{-if_{\alpha\beta}(\tau)x(\tau)} & -\chi(\tau) \end{bmatrix} \begin{bmatrix} a_\alpha(\tau) \\ a_\beta(\tau) \end{bmatrix}, \quad (25)$$

with

$$\chi(\tau) = s_{\beta p} \sigma_{\beta p} R_{\beta p} \frac{m[t(\tau)]}{1 - \Delta_{\beta p}(\tau)} \left[1 - \delta_{\beta p} \frac{1 - \Delta_{\beta p}(\tau)}{1 - \delta_{\beta p} \Delta_{\beta p}(\tau)} \times e^{-2is_{\beta p}\omega(\tau)t(\tau)} \right] [1 + e^{2is_{\beta p}\omega(\tau)t(\tau)}]. \quad (26)$$

Now a transformation of the (α, β) subsystem vector is sought

$$\begin{bmatrix} b_\alpha(\tau) \\ b_\beta(\tau) \end{bmatrix} = e^{-i\hat{\Lambda}(\tau)} \begin{bmatrix} a_\alpha(\tau) \\ a_\beta(\tau) \end{bmatrix} \quad (27)$$

with

$$\hat{\Lambda}(\tau) = \begin{bmatrix} \rho_1(\tau) & 0 \\ 0 & \rho_2(\tau) \end{bmatrix}, \quad (28)$$

such that the transformed subsystem vector satisfies

$$\frac{d}{d\tau} \begin{bmatrix} b_\alpha(\tau) \\ b_\beta(\tau) \end{bmatrix} = -i \begin{bmatrix} 0 & 1 \\ 1 & 0 \end{bmatrix} \begin{bmatrix} b_\alpha(\tau) \\ b_\beta(\tau) \end{bmatrix}. \quad (29)$$

As this equation is identical to (13), the corresponding solution would represent complete population transfer oscillations between levels α and β . Introducing transformation (27) into (25), the following equation is obtained:

$$\frac{d}{d\tau} \begin{bmatrix} b_\alpha(\tau) \\ b_\beta(\tau) \end{bmatrix} = -i \begin{bmatrix} \frac{d}{d\tau} \rho_1(\tau) & e^{i\{f_{\alpha\beta}(\tau)x(\tau) - [\rho_1(\tau) - \rho_2(\tau)]\}} \\ e^{-i\{f_{\alpha\beta}(\tau)x(\tau) - [\rho_1(\tau) - \rho_2(\tau)]\}} & -\chi(\tau) + \frac{d}{d\tau} \rho_2(\tau) \end{bmatrix} \begin{bmatrix} b_\alpha(\tau) \\ b_\beta(\tau) \end{bmatrix}. \quad (30)$$

If this is to be fitted to form (29), the following conditions must be fulfilled:

$$\frac{d}{d\tau} \rho_1(\tau) = 0, \quad (31)$$

$$\chi(\tau) - \frac{d}{d\tau} \rho_2(\tau) = 0, \quad (32)$$

$$f_{\alpha\beta}(\tau)x(\tau) - [\rho_1(\tau) - \rho_2(\tau)] = 0, \quad (33)$$

which can be compactly written as

$$\frac{d}{d\tau} [f_{\alpha\beta}(\tau)x(\tau)] = -\chi(\tau). \quad (34)$$

Integration of the last equation yields the formal solution for $\Delta_{\beta p}(\tau)$ from which optimized perturbation frequency $\omega(\tau)$ may be extracted

$$\begin{aligned} \Delta_{\beta p}(\tau) &= (s_{\beta\alpha} s_{\beta p}) \sigma_{\beta p}^2 \frac{1}{x(\tau)} \\ &\times \int_0^\tau \frac{1 - \delta_{\beta p}}{[1 - \Delta_{\beta p}(\tau')][1 - \delta_{\beta p} \Delta_{\beta p}(\tau')]} m[t(\tau')] d\tau' \\ &+ (s_{\beta\alpha} s_{\beta p}) \sigma_{\beta p}^2 \frac{1}{x(\tau)} \int_0^\tau \left[\frac{e^{2is_{\beta p}\omega(\tau')t(\tau')}}{1 - \Delta_{\beta p}(\tau')} \right] \end{aligned}$$

$$- \delta_{\beta p} \frac{e^{-2is_{\beta p}\omega(\tau')t(\tau')}}{1 - \delta_{\beta p} \Delta_{\beta p}(\tau')} m[t(\tau')] d\tau'. \quad (35)$$

Since $\Delta_{\beta p}(\tau)$ is generally a small quantity, this equation may be solved iteratively, using $\Delta_{\beta p}(\tau')=0$ as the initial value. The contribution to the total $\Delta_{\beta p}(\tau)$ from the second integral, containing rapidly rotating complex exponentials, may be shown to be minor compared to the one from the first, real integral. However, the very fact that there is an imaginary contribution to the optimized perturbation frequency indicates that the optimization procedure simply cannot completely annihilate the dynamical impact of the perturbing level. Nevertheless, as will be demonstrated in the following section, it may be done to a very good approximation.

Transforming (35) back to the original time coordinate t and keeping only the first integral yields the approximate recurrent solution for $\Delta_{\beta p}(t)$:

$$\begin{aligned} \Delta_{\beta p}(t) &= (s_{\beta\alpha} s_{\beta p}) \sigma_{\beta p}^2 (1 - \delta_{\beta p}) \frac{1}{t} \\ &\times \int_0^t \frac{[m(t')]^2}{[1 - \Delta_{\beta p}(t')][1 - \delta_{\beta p} \Delta_{\beta p}(t')]} dt'. \quad (36) \end{aligned}$$

Introducing the zeroth-order approximation $\Delta_{\beta p}(\tau')=0$ into this equation, the analytic expression for the first-order optimized frequency is obtained

$$\omega(t) = \omega_{\alpha\beta} + (\omega_{\beta p} - \omega_{\alpha\beta})(s_{\beta\alpha}s_{\beta p})\sigma_{\beta p}^2(1 - \delta_{\beta p})\frac{1}{t} \times \int_0^t [m(t')]^2 dt'. \quad (37)$$

For all but the strongest perturbations (i.e., such that $\sigma_{\beta p}^2 \sim 1$ or greater) higher-order corrections are not needed.

Note that the frequency shift in (36) and (37) may be either away from the perturbing line or towards it. Which case it will be depends on the relation between the energies of the three system levels: if level β has either the highest or the lowest total energy, so that both transitions $\beta \rightarrow \alpha$ and $\beta \rightarrow p$ are energy-wise either “downwards” ($s_{\beta\alpha} = s_{\beta p} = +1$) or “upwards” ($s_{\beta\alpha} = s_{\beta p} = -1$) then the shift will be *towards* the perturbing line; on the other hand, if the energy of level β is in between the other two energies so that these two transitions are in the opposite directions ($s_{\beta\alpha} = -s_{\beta p}$), the shift will be *away* from the perturbing line.

D. Population oscillations in the many-level system

The approach presented in Sec. II C can be easily extended to include multiple perturbation levels. The perturbation now couples each of the selected levels to a certain number of perturbing levels, and each of perturbing levels' dynamics is calculated independently from all the others. This may be done as long as the perturbation due to each single perturbing level is kept reasonably small (gauged by standards of the three-level system). Accordingly, the many-level analog of Eq. (25) is

$$\frac{d}{d\tau} \begin{bmatrix} a_\alpha(\tau) \\ a_\beta(\tau) \end{bmatrix} = -i \begin{bmatrix} -\chi_\alpha(\tau) & e^{if_{\alpha\beta}(\tau)x(\tau)} \\ e^{-if_{\alpha\beta}(\tau)x(\tau)} & -\chi_\beta(\tau) \end{bmatrix} \begin{bmatrix} a_\alpha(\tau) \\ a_\beta(\tau) \end{bmatrix} \quad (38)$$

with

$$\chi_\alpha(\tau) = m[t(\tau)] \sum_{q=1}^n s_{\alpha q} \sigma_{\alpha q} R_{\alpha q} \frac{1 - \delta_{\alpha q}}{[1 - \Delta_{\alpha q}(\tau)][1 - \delta_{\alpha q} \Delta_{\alpha q}(\tau)]}, \quad (39)$$

$$\chi_\beta(\tau) = m[t(\tau)] \sum_{p=1}^n s_{\beta p} \sigma_{\beta p} R_{\beta p} \frac{1 - \delta_{\beta p}}{[1 - \Delta_{\beta p}(\tau)][1 - \delta_{\beta p} \Delta_{\beta p}(\tau)]}, \quad (40)$$

where all quantities are defined analogously to the ones in the previous section, and complex rotating terms have been eliminated.

The many-level equivalent of (34) is

$$\frac{d}{d\tau} [f_{\alpha\beta}(\tau)x(\tau)] = [\chi_\alpha(\tau) - \chi_\beta(\tau)], \quad (41)$$

and the first-order solution is

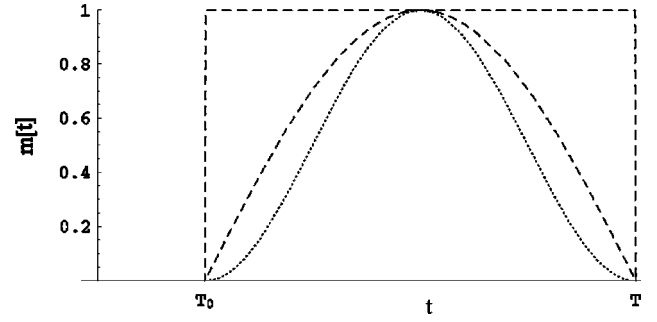


FIG. 1. Pulse envelope profiles. Time t is on the abscissa and $m(t)$ is on the ordinate. The dash-dotted line corresponds to a square pulse, the dashed line to a sine pulse, and the dotted line to a sine squared pulse. The pulse is switched on at $t=T_0$ and lasts until $t=T$. In all three cases, the maximum value of the perturbing field intensity field, F_0 , achieved at time $T-T_0/2$ is the same. In the case of the three-level system, it is such that $\sigma_{\beta p}^2 = 2.0$ while in case of the many-level system $\sigma_{\text{tot}}^2 = 0.2$.

$$\omega(t) = \omega_{\alpha\beta} + \left[\sum_{q=1}^m (\omega_{\alpha q} - \omega_{\alpha\beta})(s_{\alpha\beta}s_{\alpha q})\sigma_{\alpha q}^2(1 - \delta_{\alpha q}) + \sum_{p=1}^n (\omega_{\beta p} - \omega_{\alpha\beta})(s_{\beta\alpha}s_{\beta p})\sigma_{\beta p}^2(1 - \delta_{\beta p}) \right] \frac{1}{t} \times \int_0^t [m(t')]^2 dt'. \quad (42)$$

The total perturbation intensity for the case of a many-level system may be estimated by considering the maximum total population of all perturbing levels

$$\sigma_{\text{tot}}^2 \equiv \sum_{q=1}^m \text{Max}[\Pi_q(t; T_0 < t < T)] + \sum_{p=1}^n \text{Max}[\Pi_p(t; T_0 < t < T)] = \sum_{q=1}^m \sigma_{\alpha q}^2 + \sum_{p=1}^n \sigma_{\beta p}^2. \quad (43)$$

Hence, if $\sigma_{\text{tot}}^2 \ll 1$ the perturbation of the many-level system is small; otherwise it is large. In the following section it shall be demonstrated that (43) provides not just a qualitative, but also an excellent quantitative criterion for determination of the impact of perturbing levels on population oscillation dynamics.

III. NUMERICAL SIMULATIONS

In this section numerical simulations of system dynamics for resonant (i.e., unoptimized) and optimized [determined from (36) and (42)] perturbation frequencies are presented and compared. Several pulse envelope shapes are considered: square pulse [$m(t)=1$], sine pulse [$m(t)=\sin(\Omega t)$] and sine squared pulse [$m(t)=[\sin(\Omega t)]^2$] (Fig. 1).

A. Three-level system

First a simple three-level system is considered. In this case a full iterative solution for the optimizing driving fre-

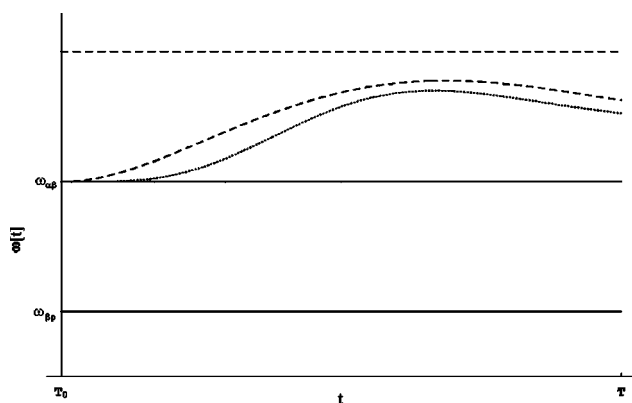


FIG. 2. Optimized frequency plots for the three-level case. Time t is on the abscissa, the perturbation frequency $\omega(t)$ on the ordinate. The total pulse duration is 7.25 ns. Two straight solid lines indicate the two resonant frequencies of the system, $\omega_{\beta\alpha}$ (upper) and $\omega_{\beta p}$ (lower). The remaining three lines are optimized frequencies for the three types of pulse: the dash-dotted for a square pulse, the dashed line for a sine pulse, and the dotted for a sine squared pulse.

quency is easy to calculate from Eq. (35) (with complex contributions neglected). System parameters have the following values (a.u. \equiv atomic units): $\omega_{\beta\alpha}=0.017\ 671$ a.u., $s_{\beta\alpha}=1$, $\mu_{\beta\alpha}=0.073$ a.u., $\omega_{\beta p}=0.017\ 611$ a.u., $s_{\beta p}=-1$, $\mu_{\beta p}=0.098$ a.u.. These system parameters correspond to the

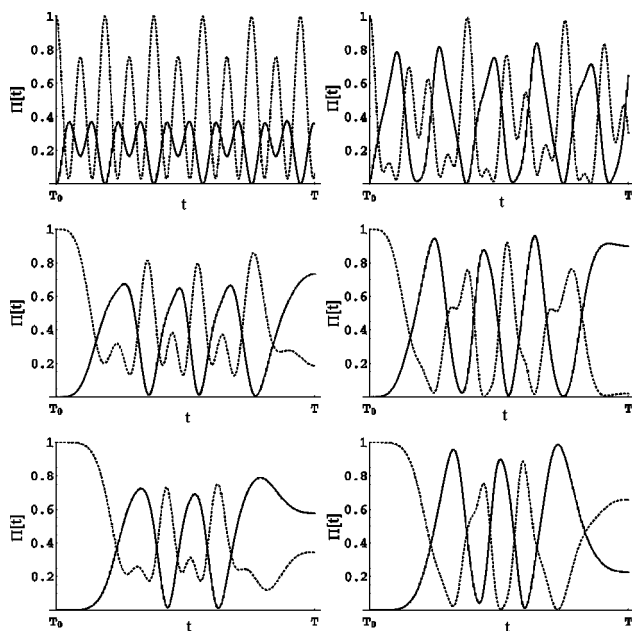


FIG. 3. Comparison of the resonant and optimized population dynamics. Graphs on the left side present numerical solution to system dynamics for each of pulse types with a resonant perturbation applied, $\omega(t)=\omega_{\beta\alpha}$. Graphs on the right-hand side present optimized dynamics. The top row corresponds to a square pulse, the middle to a sine pulse, and the bottom row to a sine square pulse. For the sake of clarity, only α (solid line) and β (dashed line) populations are plotted while p population is omitted. Although the optimization clearly does not produce clean two-level dynamics, the increase in the amplitude of population oscillation is nevertheless evident.

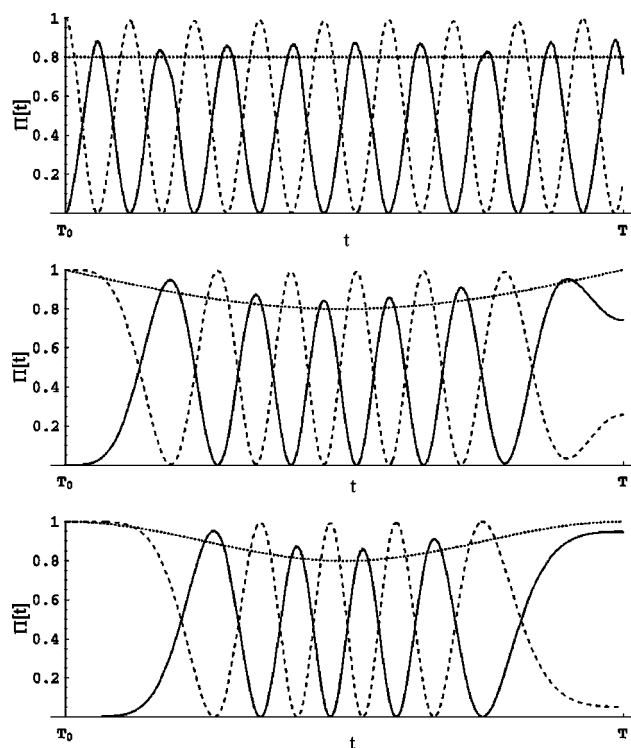


FIG. 4. Optimized population dynamics of the two targeted levels in the many-level system. Time t is on the abscissa, populations $\Pi_{\alpha,\beta}(t)$ are on the ordinate. The top graph corresponds to a square pulse, the middle to a sine pulse and the bottom one to a sine squared pulse. In all cases $\sigma_{\text{tot}}^2=0.2$ and the total duration of the pulse is 4.84 ns. The dotted line on each graph indicates the function $1-m(t)\sigma_{\text{tot}}^2$.

three rovibrational levels of the HF molecule in the ground electronic state: $\alpha \equiv (v=0, j=2, m=0)$, $\beta \equiv (v=1, j=1, m=0)$, $p \equiv (v=2, j=2, m=0)$. System parameters are such that the optimizing frequency shift is away from the perturbing line. In all cases, the total pulse duration $T-T_0$ equals 7.25 ns.

In order to present clearly the improvement that optimization of driving frequency induces in population transfer between the two selected levels, the perturbation strength in following examples is set to an extreme value: $\sigma_{\beta p}^2=2.0$. Figure 2 compares evolution of optimized frequency $\omega(t)$ with two resonant frequencies of the system, $\omega_{\beta\alpha}$ and $\omega_{\beta p}$. In Fig. 3 resonant and optimized population dynamics are shown for each of envelope shapes. The increase in the amplitude of the population transfer between the selected two levels is obvious.

B. Many-level system

As an example of a many-level system, the set of rovibrational states of the HF molecule in the electronic ground state is considered. The numerical model used for the calculation of the system dynamics includes 310 levels (31 rotational \times 10 vibrational). It is based on the HF inter-nuclear potential data and electric dipole moment data from [10,11], respectively. The targeted transition is $(v=1, j$

$=1, m=0) \rightarrow (v=0, j=0, m=0)$. In all cases, the total pulse duration $T-T_0$ equals 4.84 ns.

It was demonstrated in the previous subsection that optimization indeed leads to improvement of the population transfer dynamics, even when the perturbation is very large. However, as in such conditions complete population transfer is unattainable, these examples were more of a qualitative nature from the standpoint of population transfer control. The many-level system considered now is more realistic than the previous three-level one and the focus is shifted to quantitative predictions. Hence, the employed drive intensity will be much smaller so that results can be directly applied to population transfer control. Pulse envelope shapes are the same as in the three-level case (see Fig. 1). Maximum amplitudes of electric field are likewise equal in all three cases, but now they are chosen so that $\sigma_{\text{tot}}^2=0.2$. Since the perturbation is relatively small, the optimized frequency may be determined from the first-order approximate solution (42).

In Fig. 4 the optimized dynamics of two target system levels is shown for each of three pulse envelopes. In all cases two things should be noted. First, the general shape of the optimized dynamics of each of the two selected levels is fairly close to pure sinusoidal oscillations. This is more so, the smaller the perturbation strength parameter σ_{tot}^2 is. However, the complete population transfer is again not achieved because a certain share of the population unavoidably ends up in perturbing levels. Second, the actual instantaneous loss of population transfer is close to (and actually smaller than) $m(t)\sigma_{\text{tot}}^2$, as indicated by dotted line in each of the plots. This shows that σ_{tot}^2 indeed is a good quantitative (and not just qualitative) indicator of relative drive strength. The argument which led to relation (24) may, hence, again be applied to determine the maximum intensity of the driving radiation to be employed if population losses to perturbing levels are to be smaller than some predefined amount.

IV. CONCLUSION

As was stated in the introduction, the aim of this paper is to explore and refine the use of Rabi oscillations as a tool in

selective population manipulation of complex discrete-level quantum systems. The main aims of such manipulation are as great as possible population transfer and at the same time as short as possible population transfer time. From the simple two-level theory it is well known that the an increase in drive intensity yields a reduction in population oscillation period. However, the same theory can neither fully disclose all the limitations of this result that arise from the complexity of the internal structure of a many-level system, nor can it handle the unavoidable loss of population to the rest of the system. Results presented in this paper fill this gap: they enable one to determine the maximum possible drive intensity (and hence the lower limit of time) with which oscillations of preselected amplitude (say 99%) may be achieved, and at the same time to minimize unavoidable losses of the population to nontargeted system levels. Finally, the method of Rabi spectra (see Ref. [9]) presents a simple, yet useful conceptual supplement to the analysis presented in this paper.

In order to achieve the quickest possible population transfer between two preselected levels, driving pulse should be tailored so that it produces only a single half oscillation of the population. However, during research for this paper it has been noted that for strong fields standard π -pulse theory see Eq. (14) and Ref. [12] is also deficient when it comes to the complex many-level systems. Work is currently in progress on analytical extension of standard π -pulse theory that would resolve this issue.

ACKNOWLEDGMENTS

The author is very grateful to Dr. Nadja Došlić for insightful discussions and assistance during work on problems explored in this paper. The author is also grateful to Dr. Danko Bosanac for providing the initial idea from which the topic of this research developed.

-
- [1] G. Paramonov and V. Savva, Phys. Lett. **97A**, 340 (1983).
 - [2] S. Chelkowski, A. Bandrauk, and P. Corkum, Phys. Rev. Lett. **65**, 2355 (1990).
 - [3] M. Kaluza, J. Muckerman, P. Gross, and H. Rabitz, J. Chem. Phys. **100**, 4211 (1993).
 - [4] K. Bergmann, H. Theuer, and B. Shore, Rev. Mod. Phys. **70**, 1003 (1998).
 - [5] H. Rabitz, Science **299**, 525 (2003).
 - [6] M. Shariar and P. Pradhan, e-print quant-ph/0212121.
 - [7] J. Barata and W. Wreszinski, Phys. Rev. Lett. **84**, 2112 (2000).
 - [8] K. Fujii, e-print quant-ph/0301145.
 - [9] D. Bonacci, e-print quant-ph/0309126.
 - [10] H. Mueller *et al.*, Theor. Chem. Acc. **100**, 85 (1998).
 - [11] W. Zemke, W. Stwalley, S. Langhoff, G. Valderama, and M. Berry, J. Chem. Phys. **95**, 7846 (1991).
 - [12] M. Holthaus and B. Just, Phys. Rev. A **49**, 1950 (1994).